Parallel dual secondary column-dual detection: a further way of enhancing the informative potential of two-dimensional comprehensive gas chromatography

Luca Nicolotti[1], Chiara Cordero[2*], Davide Bressanello[2], Cecilia Cagliero[2], Erica Liberto[2], Federico Magagna[2], Patrizia Rubiolo[2], Barbara Sgorbini[2] and Carlo Bicchi[2]

[1]Author's affiliation:
Faculty of Chemistry, Technical University of Munich; Lise-Meitner-Strasse 34, 85354 Freising, Germany

[2]Authors' affiliation:
Dipartimento di Scienza e Tecnologia del Farmaco, Università di Torino, Via Pietro Giuria 9, I-10125 Turin, Italy

* Address for correspondence:
Dr. Chiara Cordero - Dipartimento di Scienza e Tecnologia del Farmaco, Università di Torino, Via Pietro Giuria 9, I-10125 Torino, Italy – e-mail: chiara.cordero@unito.it ; phone: +39 011 6707662; fax: +39 011 2367662

Abstract

Comprehensive two-dimensional gas chromatography (GC×GC) coupled with Mass Spectrometry (MS) is one of today's most powerful analytical platforms for detailed analysis of medium-to-high complexity samples. The column set usually consists of a long, conventional-inner-diameter first dimension (^{1}D) (typically 15-30 m long, 0.32-0.25 mm d_c), and a short, narrow-bore second dimension (^{2}D) column (typically 0.5-2 m, 0.1 mm d_c) where separation is run in a few seconds. However, when thermal modulation is used, since the columns of a set are coupled in series, a flow mismatch occurs between the two dimensions, making it impossible to operate simultaneously at optimized flow conditions. Further, short narrow-bore capillaries can easily be overloaded, because of their lower loadability, limiting the effectiveness of ^{2}D separation.

In this study, improved gas linear velocities in both chromatographic dimensions were achieved by coupling the ^{1}D column with two parallel ^{2}D columns, having identical inner diameter, stationary phase chemistry, and film thickness. In turn, these were connected to two detectors: a fast quadrupole Mass Spectrometer (MS) and a Flame Ionization Detector (FID). Different configurations were tested and performances compared to a conventional set-up; experimental results on two model mixtures (*n*-alkanes and fourteen medium-to-high polarity volatiles of interest in the flavor and fragrance field) and on the essential oil of *Artemisia umbelliformis* Lam., show the system provides consistent results, in terms of analyte identification (reliability of spectra and MS matching) and quantitation, also affording an internal cross-validation of quantitation accuracy.

Key-words:

Two-dimensional comprehensive gas chromatography-mass spectrometry; parallel dual secondary column-dual detection; dual ^{2}D pattern alignment, outlet pressure correction, second dimension linear velocity optimization, essential oil analysis

1. Introduction

Comprehensive two-dimensional gas chromatography (GC×GC) coupled with Mass Spectrometry (MS) is one of the most powerful analytical platforms now available for the detailed analysis (identification and quantitation) of medium-to-high complexity samples. Compared to one-dimensional systems, it offers remarkable separation power and unmatched peak capacity [1,2]; the possibility of applying different separation mechanisms in the two chromatographic dimensions produces rationalized 2D patterns, suitable as sample fingerprints for classification and identification purposes [3].

The most common GC×GC column sets consist of a long, conventional-inner-diameter first dimension (^{1}D) (typically 15-30 m long and 0.32-0.25 mm d_c), and a short, narrow-bore second dimension (^{2}D) column (typically 0.5–2 m 0.1 mm d_c). Thanks to the short narrow-bore ^{2}D column, the separation is run in a few seconds, both minimizing wrap-around phenomena and contributing to the high efficiency of the system. However, when thermal modulation is used, since the columns of a set are coupled in series, a flow mismatch occurs between the two dimensions; this makes it impossible to operate simultaneously at optimized flow conditions. In addition, short narrow-bore capillaries can easily overload, because of their lower loadability, limiting ^{2}D separation effectiveness [4,5]. The configuration and optimization of a GC×GC set-up is thus a crucial, but also a complex step, since separation in the two dimensions is differently influenced in the two separation dimensions by carrier gas flow, temperature, and modulation period. With regard to the flow regime, in their earlier publications Phillips *et al* [6,7] indicated a possible way of optimizing carrier gas flow by splitting part of the flow from ^{1}D to waste, prior to modulation. They adopted a Tee union to connect the two analytical columns, and a short capillary segment enabling the diversion of about 30% of the primary column flow to waste, thus applying flows closer to the optimal in both dimensions, and reducing overloading of the ^{2}D.

In 2007, Tranchida *et al.* [8] included a flow splitter in a classical GC×GC-FID system. The method, called "split-flow" comprehensive 2D-GC, consisted of a ^{1}D apolar 30 m × 0.25 mm d_c column, connected to a 1 m × 0.10 mm d_c polar ^{2}D and to an uncoated capillary of 30 cm × 0.10 mm d_c, using a Y press fit. The carrier gas (hydrogen) linear velocities were regulated thanks to a manually-operated split valve, connected to the uncoated capillary. Experimental results on Fatty Acids Methyl Esters (FAMEs) from a cod oil sample showed that, with a 35:65 (FID) split-flow ratio and 146.3 kPa head pressure, gas velocities close to optimal could be obtained (i.e., about 35 and 213 cm/sec in the ^{1}D and ^{2}D respectively) with a positive effect on separation efficiency and resolution (+50% for a selected critical pair) while maintaining structured chromatograms.

Other straightforward solutions have been proposed to overcome this critical issue, which is known as flow-mismatch in the two dimensions. In stop-flow GC×GC [9-11] the ^{1}D flow is periodically halted and during each pause the ^{2}D separation continues, by delivering carrier gas via an auxiliary pressure controller. This

latter set-up enables column flow to be independently regulated, thus optimizing the separation in both dimensions.

Another possibility is to adopt wider ^{2}D capillaries [12,13]; if columns of a set have the same inner diameter, flow conditions closer to optimal can be applied in both dimensions, improving the exploitation of the ^{2}D stationary phase selectivity, even at higher temperature rates, and at the same time increasing ^{2}D column loadability [12]. Experimental results on medium-complexity samples of interest in the flavor and fragrance field, with homologous d_c column sets, show that the mean loss of peak capacity (by a factor of 3; System Separation Measure - $S_{GC\times GC}$) is partially or fully compensated, thanks to better exploitation of ^{2}D stationary phase selectivity. At the same time, reliable quali-quantitative results are achieved, by complying with the minimal modulation requirements (Modulation Ratio criterion - M_R) [13]. More recently, Peroni *et al.* evaluated two alternative solutions: (*a*) the use of monolithic ^{2}D columns [14], and (*b*) multiple capillary columns in parallel as ^{2}D [15]. With monoliths, efficiency and column flow can be optimized independently, but at the cost of poor separation efficiency. However, multi-^{2}D columns appear to be a good alternative; the carrier gas flow is divided over multiple-parallel ^{2}D flow paths, enabling both dimensions to be fully exploited at the same time. Unfortunately, as the authors themselves state, coupling the ^{1}D to the multi-^{2}D is, in practice, rather a complex procedure, limiting the feasibility of such set-ups in routine use.

As discussed by Peroni and Janssen [16], the optimum linear velocities in both dimensions are reduced when the second dimension operates at high outlet pressure. The proposed set-up includes a restrictor at the outlet of the ^{2}D, prepared by melting the end of the column with a high-temperature hydrogen flame (1800°C) until closure, and then partially re-opening it, by grinding it with sandpaper, to obtain the desired flow. The elevated outlet pressure conditions resulted in flatter *Van Deemter* curves at higher velocities, causing a slower loss of efficiency at higher inlet pressures. Experimental results indicated that this system configuration is characterized by a slightly improved resolution for a given column set, compared to conventional pressure drops, but that the analysis time is longer.

In the present study, improved gas linear velocities in both chromatographic dimensions were achieved by coupling the ^{1}D column with two parallel ^{2}D columns having identical inner diameter, stationary phase chemistry, and film thickness, in turn connected to two detectors: a fast quadrupole Mass Spectrometer (MS), and a Flame Ionization Detector (FID). The system was equipped with a loop-type thermal modulator; cryotrapping and refocusing were set at the head of the ^{2}D capillaries to narrow bands entering the ^{2}D [17]. Three different column set-up were tested: the first, *Set-up I*, included a primary column connected with two parallel ^{2}Ds of different lengths (1.6 m x 0.1 mm d_c to MS and 1.4 m x 0.1 mm d_c to FID) but operating at an almost equal nominal flow (comparable hold-up times) although subjected to different outlet pressures. The second system configuration, *Set-up II*, included two identical ^{2}D columns (1.4 m x 0.1 mm d_c) and an auxiliary pressure controller to deliver a supplementary flow of carrier gas at the outlet of the ^{2}D connected to the MS detector. The latter was inspired by the system proposed by Shellie *et al.* [18],

in which GC×GC-FID and GC×GC-TOF-MS chromatograms were successfully matched, obtaining almost identical 2D patterns thanks to the adjustment of inner and outlet pressures. Lastly a conventional set-up was taken as a reference, i.e. *Set-up III* consisted of a single ^{2}D column (total length including modulation loop: 1.4 m x 0.1 mm d_c) connected to two parallel detectors, via splitting capillaries.

The performance of each *Set-up* are evaluated by analyzing two model mixtures (n-alkanes (HydStd1) and 14 medium-to-high polarity volatiles in the flavor and fragrance field (FFStd2)), and the *Artemisia umbelliformis* Lam. essential oil. The potentials and limits of each set-up are also discussed in terms of separation performances and in view of the practical information that can be derived from each single analytical run.

2. Experimental

2.1 Samples and solvents

Pure standards of *n*-alkanes (from *n*-C9 to *n*-C25) for system evaluation, flow/pressure optimization and Linear Retention Indices (I^T_S) determination were from Sigma-Aldrich (Milan, Italy).

Pure standards of α-pinene, benzaldehyde, benzyl alcohol, α-thujone, camphor, carvone, cinnamyl alcohol, geranyl acetate, vanillin, coumarin, isoeugenol, isoeugenyl acetate, benzyl benzoate, and sclareol, were from Sigma-Aldrich (Milan, Italy). The two model mixtures (i.e., HydStd1 and FFStd2) for system evaluation were prepared by mixing single component Standard Mother Solutions, at 10 g/L in dichloromethane, and adjusting the final volume up to 100 mg/L. Solvents were all HPLC-grade, from Riedel-de Haen (Seelze, Germany).

Artemisia umbelliformis Lam. essential oil (EO) was prepared following the method of the European Pharmacopoeia [19]. Ten grams of dried aerial parts from experimental cultivations run in different alpine valleys were suspended in 250 mL of water in a 500 mL flask for 1 h, and then submitted to hydrodistillation in a Clevenger micro-apparatus for 2 hours [20]. The resulting EO was left to stabilize for 1 h, then recovered and analyzed directly.

2.2 GC×GC instrument set-up

GC×GC analyses were run with a system configured as follows: a HT280T multipurpose sampler (HTA, Brescia, Italy) was integrated with an Agilent 6890 GC unit coupled to an Agilent 5975C MS detector (Agilent, Little Falls, DE, USA) operating in EI mode at 70 eV. The GC transfer line was set at 280°C. A *Standard Tune* was used and the scan range was set to m/z 40-300 with a scanning rate of 12,500 amu/s to obtain a spectra generation frequency of 28 Hz. The Flame Ionization Detector (FID) conditions were: base temperature 280°C, H_2 flow 40 mL/min; air flow 240 mL/min; make-up (N_2) 450 mL/min; sampling frequency 150 Hz.

153 Injections of the essential oil, and of the two model mixtures, as well as those for I^T_S determination
154 samples, were by HT280T sampler (HTA, Brescia, Italy) under the following conditions: split/splitless
155 injector, split mode, split ratio 1/50, injector temperature 280°C, injection volume 0.1 µL of undiluted
156 essential oil and 1µL of the *n*-HydStd1 and FFSTd2 model mixtures at 100 mg/L. The oven temperature was
157 programmed as follows: 50°C (1 min) to 270°C at 3.0°C/min and to 290°C at 10°C/min (10 min).
158 Flow/pressure optimization was checked on a standard solution of tridecane, tetradecane and pentadecane
159 (n-C13 to n-C15) at 100 mg/L analyzed in isothermal conditions at 150°C. Head-pressure values are
160 reported in **Table 1.**
161
162 **2.3 Thermal modulator parameters**
163 The system was equipped with a two-stage KT 2004 loop thermal modulator (Zoex Corporation, Houston,
164 TX) cooled with liquid nitrogen controlled by Optimode™ V.2 (SRA Instruments, Cernusco sul Naviglio, MI,
165 Italy). Hot jet pulse time was set at 250 ms, modulation time was 5 s and cold-jet total flow progressively
166 reduced with a linear function, from 40% of Mass Flow Controller (MFC) at initial conditions, to 5% at the
167 end of the run. Loop dimensions were chosen on the basis of the expected carrier linear velocities, to
168 ascertain that at least two stage-band-focusing releases were performed for each modulation. Thus, for all
169 *Set-ups,* the first 0.6 m of the ^{2}Ds war wrapped in the metal slit of the modulator.
170
171 **2.4 Column connections and auxiliary control module**
172 Connections between the primary and the two secondary columns (*Set-ups I* and *II*), and between the
173 secondary column and the deactivated capillaries for FID/MS effluent splitting (*Set-up III*) was via a SilFlow™
174 GC 3 Port Splitter (SGE Ringwood, Victoria, Australia). The auxiliary pressure controller consisted of a one
175 channel Pneumatics Control Module (G2317A) connected to a Quick Swap unit (G3185, Agilent, Little Falls,
176 DE, USA) with a restrictor capillary of 0.17 m x 0.1 mm d_c. A diagram of the system configuration is provided
177 as Supplementary File (Supplementary Figure 1 - SF1).
178 Column set configurations are listed in **Table 1,** together with carrier gas head pressures and calculated
179 linear velocities [18,21].
180
181 **2.5 Data acquisition and 2D plot elaboration**
182 Data were acquired by Agilent MSD ChemStation ver D.02.00.275 and processed using GC Image GC×GC
183 Software version 2.1b1 (GC Image, LLC Lincoln NE, USA).
184
185 **3. Results and discussion**
186 **3.1 Some theoretical aspects**

Conventional GC×GC configurations with thermal modulators imply that the two columns of the set are connected in series and the volumetric flow rates and linear velocities in the two capillaries are correctly calculated; the pressure drop across the total length must also be estimated [8,18] ,.

The outlet column volumetric flow ($F_{o(C)}$) can be derived by the Poiseulle equation (Eq. 1)

$$F_{o(C)} = \frac{60\pi r^4}{16\eta L}\frac{(p_i{}^2 - p_o{}^2)}{p_o}\frac{T_{ref}}{T} \qquad \text{Equation 1}$$

where r is the column radius, η the dynamic viscosity of the carrier gas at a given temperature, L is the column length, p_i and p_o are the absolute inlet and outlet pressures, and T_{ref} is the reference temperature (typically 298K) and T is the absolute operative temperature.

The pressure at any point (z) along the column can be calculated according to Equation 2:

$$p_z = \sqrt{p^2 - \left(\frac{z}{L}\right)(p^2 - 1)} \qquad \text{Equation 2}$$

The linear velocity at the column outlet (u_o) is:

$$u_o = \left(\frac{r^4 (p_i^2 - p_o^2)}{16\eta L p_o}\right) \qquad \text{Equation 3}$$

where r is the column radius, η the dynamic viscosity of the carrier gas at the operating temperature, L is the column length, p_i and p_o are the absolute inlet and outlet pressures. The average velocity is proportional to the outlet velocity corrected by the compression factor *j:*

$$\bar{u} = u_o \cdot j \qquad \text{Equation 4}$$

where

$$j = \frac{3}{2}\frac{(p^2-1)}{(p^3-1)} \qquad \text{Equation 5}$$

The average linear velocity along each separation dimension can be estimated by combining the above functions. **Table 1** reports average linear velocities, calculated at 333 K (60°C), together with inlet pressure (p_i), midpoint pressure (p_2) at the connection between primary and secondary column(s) in kPa (over pressure) and hold-up times (s). In the case of *Set-up II,* the data do not include the adjustment of outlet pressure by the auxiliary flow controller.

3.2 Parallel dual secondary columns operating at different outlet pressures (GC×2GC-MS/FID)

The first part of this study was carried out on dual parallel columns of identical inner diameter (i.e., 0.10 mm d_c) but of an almost equivalent length in terms of flow resistance. *Set-up I* was inspired by the "split-flow" configuration proposed by Tranchida *et al.* [17], with the sole difference that the outlet of the split capillary (an OV1701 capillary column with 0.10 µm d_f) was connected to a FID detector (atmospheric pressure). Compared to a conventional configuration (*Set-up III*), where one of the two dimensions has to operate very far from its optimum performance, whatever the head pressure, in *Set-up I* close-to-optimal linear velocities in both chromatographic dimensions are applied, i.e. ^{1}D at about 34 cm/s and the ^{2}Ds at about 180 cm/s(see **Table 1**).

Differences in secondary column length were expected to condition the separation in terms of absolute retention and peak-widths. However, the resulting 2D patterns were expected to be consistent, although not identical. According to Schutjes *et al.* [21], who rearranged the *Golay* plate height equation in terms of dimensionless parameters (i.e., $\xi=H/H_{min}$ and $\nu=\bar{u}/\bar{u}_{opt}$), operating at p_i/p_o >>1 (i.e., vacuum outlet), the maximum efficiency is reached for a close interval of average linear velocities around $\bar{u}_{opt}$. Conversely, when p_i/p_o approaches unity (i.e. at ambient pressure), the experimental curve of H/H_{min} as a function of $\bar{u}/\bar{u}_{opt}$ is flatter, and enables a better separation efficiency. With *Set-up I* lower efficiencies were expected for the MS branch [21] also in consequence of the longitudinal diffusion effect.

The experimental results confirmed these hypotheses: **Figure 1** shows the raw chromatogram overlaid with 2D plots of linear hydrocarbons from C13 to C15 analyzed in isothermal conditions (i.e., 150°C) at 296 kPa head-pressure with *Set-ups I* and *II*. System hold-up times, measured experimentally with methane injections at 80% of MFC cold jet regulation, were 1.905 min and 0.86 s in the ^{1}D and ^{2}D respectively, in fair accordance with the expected values. Alkanes showed an absolute retention time shift (MS *vs.* FID) of -0.18 s for n-C13 and of -0.36 s for n-C15. Although minimized by the lower retention in the second dimension due to the temperature of the isothermal analysis, a much larger mismatch was expected for temperature programmed conditions and strongly retained analytes.

Figure 2 reports 2D plots (**Fig. 2a** full scan MS and **Fig. 2b** FID plots) of *Artemisia umbelliformis* essential oil, analyzed with *Set-up I*. The consistency of the 2D patterns of the two detectors is evident; the structured patterns of mono-terpenoid (*m*) and sesqui-terpenoid (*s*) hydrocarbons are clearly organized, and separated from the oxygenated derivatives (*mox* and *sox*) and from other secondary metabolites (mono terpenoid esters - *mest*). More polar compounds (carbonyl derivatives, alcohols and esters) having greater affinity for the second dimension stationary phase were more strongly retained along the ^{2}D branch towards MS (higher retention factors - *k*).

The magnitude of the retention time shift is better illustrated in **Figures 3a** and **3b,** which show ^{2}D retention time absolute differences (FID *vs.* MS) for: (**3a**) *n-alkane* hydrocarbons from *n*-C9 to *n*-C25 and (**3b**) fourteen volatiles of interest in flavor and fragrance applications. For the *n*-alkanes, where retention in the ^{2}D is negligible, absolute differences in retention times in no case exceeded (-)0.15 s (i.e., 3% as relative %

difference over 5 seconds of ^{2}D separation time); conversely, ^{2}D retention shifts for more polar compounds (**Fig. 3b**) were larger with differences between MS and FID patterns ranging from the (-)0.12 s of α-pinene to the (-) 0.68 s of vanillin (i.e., 2.38 and 13.6 % of relative difference). Marked differences were recorded for the more polar analytes (benzyl alcohol, cinnamyl alcohol, vanillin, isoeugenol and isoeugenyl acetate) that suffered from the wrap-around phenomenon.

3.3 Parallel dual secondary columns operating at equivalent (atmospheric) outlet pressures (GC×2GC-MS/FID)

The study continued, adopting two secondary columns with the same number of theoretical plates and the same equivalent lengths, in terms of flow resistance; in addition a correction of the pressure drop across dimensions was operated by an auxiliary flow/pressure controller (EPC) connected to a microfluidic device installed between the outlet of the $^{2}D_{MS}$ column and the MS transfer line (restrictor) [18].

In *Set-up II*, the two ^{2}D columns were both 1.4 meters long (0.6 meters at the head of each column were wrapped to form the modulation loop) thus leaving available 0.8 meters of each column for separation. At the end of the ^{2}D to MS, 0.17 m x 0.1 mm d_c of deactivated silica capillary (restrictor) was used to compensate for differences in flow resistance (**Table 1**: *Set-up II* - auxiliary off conditions). Additional helium flow was delivered by setting the auxiliary EPC at 40 kPa (5.7 psi relative) to adjust the outlet pressure towards MS. The compensation was minimal, because of the low resistance of the two parallel ^{2}Ds.

The outlet pressure correctness was verified by isothermal analysis (i.e., 150°C) of linear hydrocarbons from C13 to C15 at 296 kPa head-pressure; **Figure 1b** shows the raw chromatograms overlaid with the FID ^{2}D plot resulting from an outlet pressure correction towards MS of 40 kPa. System hold-up times were 1.91 min and 0.88 s in the ^{1}D and ^{2}D respectively. Alkanes did not show any retention time shift. Experiments without outlet pressure correction were also run with test mixtures and under programmed temperature conditions; the relative difference between ^{2}D retention times was on average 0.6 % for *n*-alkanes and 5.65 % for the FFStd2 model mixture. Figures **3c** and **3d** show absolute differences in time values in detail. Again, wrapped-around analytes showed higher discrepancies between ^{2}D elution times, due to accumulation of the delay error across subsequent modulations. However, with pressure compensation, the retention shift in no case exceeded 1.1 % for linear hydrocarbons and 4% (cinnamyl alcohol) for the FFStd2 model mixture components. These values are in agreement with those reported by Shellie *et al.* [18], although most of the analytes investigated in that study had lower retention in both dimensions.

Figures 2c and **2d** show the 2D plots (**Fig. 2c** full scan MS and **Fig. 2d** FID plot) of *Artemisia umbelliformis* essential oil, analyzed with *Set-up II* with auxiliary outlet compensation. As is clear, the 2D patterns are in this setup highly consistent, the structure is maintained, and the chromatographic space properly occupied. Experiments run without any outlet pressure correction (data not shown) produced 2D patterns with very

few differences from those shown, and this approach would be a good alternative when an additional EPC is not available, or turbo pumping systems do not tolerate high outlet flows. In such cases, adaptive algorithms (called *transforms*) for pattern recognition, like those used for template matching procedures [23] in targeted and untargeted data elaboration, can successfully compensate for ^{2}D retention times shifts, and consistently transfer identification from MS to FID.

3.4 Single secondary column with dual parallel detection (GC×GC-MS/FID)

To evaluate the practical advantages that can be obtained by operating at near-optimal linear velocities, with two parallel columns and two detection systems, an additional setup (*Set-up III*) consisting of a single ^{2}D column (1.4 m x 0.1 mm d_c) connected to two parallel detectors was tested. Pressure/flow conditions adopted were a compromise between optimal conditions in both dimensions, and were allowed to run at 23 cm/s and 240 cm/s in the ^{1}D and in the ^{2}D, respectively. As expected, with *Set-up III* ^{1}D retention times slightly increased, reflecting the higher elution temperatures that resulted, while those in the ^{2}D decreased, due to the consequent loss of retention. **Figures 4a**, **4b** and **4d** show differences in retention times from *Set-up I* to *Set-up III*.

For *Artemisia umbelliformis* essential oil, although the separation structure was maintained, the overall resolution was lower. **Figures 2e** and **2f** show the 2D patterns resulting from *Set-up III*. In this case, a concurrent reduction of the temperature rate and of the modulation period might be expected to produce better results, although analysis time is longer.

3.5 Practical advantages of the optimized GC×2GC-MS/FID platform

Some aspects deserve a brief discussion, to outline the practical advantages on real-world samples deriving from a GC×2GC-MS/FID platform, in terms of both dual ^{2}D column and dual detection. *Artemisia umbelliformis* essential oil was selected as a case study, since its detailed quantitative profiling is interesting for botanical classification, as well as in the light of quality aspects relating to its use to prepare a highly-prized Alpine liqueur, called “genepì”, characterized by a bitter taste and a distinctive aroma [24]. These sensory properties can be ascribed to terpenoids, in particular to α- and β-thujones, the main components of the volatile fraction for the aroma profile, and to sesquiterpene lactones with a *cis*-eudesmanolide skeleton (5-desoxy-5-hydroperoxy-5-epitelekin; 5-desoxy-5-hydroperoxytelekin and umbellifolide) for its bitterness [25]. The debate on the toxicity of thujones is still open [26], and European Union legislation has fixed a limit of 35 mg/kg on the total amount of these compounds in alcoholic beverages [27]. Thujone-free chemotypes of *A. umbelliformis* have been selectively bred to overcome this issue, and diagnostic fingerprints have been defined by combining biomolecular characterization with chemical profiling of informative secondary metabolites [25]. In any case, a detailed profiling of the volatile fraction is necessary to assess both sensory quality and safety of the aerial parts that are used to prepare the liqueur.

The first aspect to be considered is the separation power of GC×2GC-MS/FID. Resolution reflects the adequacy of the separation conditions adopted for a given group of target analytes, and becomes fundamental for samples where several informative peaks in variable abundances elute in a given region of the chromatographic space. Extra-chromatographic phenomena, e.g. column overloading, may in these cases condition correct separation, i.e. identification/quantitation. For example, when ^{2}D overloading occurs, minor peaks eluting in the proximity of highly abundant components, with large peak-width, may be lost, together with the information they carry. The ^{2}D dual column doubles the ^{2}D loadability, thus limiting ^{2}D overloading and loss of significant minor peaks due to this phenomenon. At the same time, the higher efficiency due to the average linear velocity closer to the optimal value, and the enhanced ^{2}D stationary phase selectivity, increase the system orthogonality, improving occupation of the chromatographic plane. For instance, the calculated α-thujone half-height peak width in the FFStd2 model mixture at 100 mg/L, was 120 ms (see **Table 2**). In *A. umbelliformis* essential oil, α- and β-thujones are the two most abundant peaks, each with a peak width of 480 ms, that dramatically overloads the ^{2}D; in *Set-up III*, where the second dimension loadability is halved compared to *Set-up II*, they coelute in ^{1}D-GC with two minor components, i.e. nonanal and 2-methylbutyl isovalerate. Apparent resolution values (*R*) estimated on the raw chromatogram, and referred to the most abundant modulation for all compounds, were 1.93 for the 2-methylbutyl isovalerate/α-thujone pair with *Set-up II,* and 1.53 with *Set-up III,* while for the nonanal/α-thujone pair they were 1.28 for *Set-up II*, but coeluted in Set-up III (**Figure 5**).

A second practical aspect to consider for in attempting an overall evaluation of the potential of a GC×2GC-MS/FID system concerns quantitation reliability: this exploits the synergisms of dual detection operating by different principles. MS is known to provide a fundamental contribution to unequivocal analyte identification, while FID offers a wide dynamic range of linearity and a very high frequency of acquisition, thereby improving the accuracy of 2D peak (areas) volumes. Moreover, the correct alignment of the two patterns obtained with both *Setup II* and *Setup III* enables one to consider the data set from the two detectors as a single integrated system, thus cross-validating the results. These considerations are confirmed by experimental data on the FFStd2 mixture. **Table 2** shows ^{1}D and ^{2}D retention times and their absolute errors (^{2}D Error in seconds), Normalized 2D Volumes for MS (TIC current) and FID signals (normalization was done on geranyl acetate), half-height peak-width (50% peak width (ms)) and the number of points per peak (MS operated at 28 Hz and FID at 150 Hz) for the analytes of FFStd2 mixture with *Set-up II* and *Set-up III*.

These results demonstrate that the chromatographic efficiency (expressed as half-height peak-width) is comparable for the two setups. It has to be stressed that *Set-up III* had to operate at ^{2}D flow conditions close to those adopted for the two-parallel-column system; if higher head-pressures had been applied, peak-widths would have been narrower. The number of points-per-peak was, in consequence, similar for

Setup II and *Setup III* for each detector, while mass quantitative descriptors (Normalized 2D Volumes) from the two detectors were consistent.

However, the potential of dual detection can concretely be perceived with real-world samples (e.g. *A. umbelliformis* essential oil). In these applications, the consistency of acquired MS spectra is fundamental since identification is mainly based on commercial spectral libraries. **Table 3** reports the ^{1}D Linear Retention Indices (experimental and reference values [28]), the MS match factors resulting from the NIST Identity Spectrum Search algorithm (NIST MS Search 2.0 ver. d) on spectra collected in commercial databases, and/or on spectra obtained by analyzing reference compounds, and the Signal-to-Noise (Peak-to-Peak S/N as calculated by the Agilent algorithm - SNR) estimated on the highest modulation of each 2D peak of the components characterizing *A. umbelliformis* essential oil.

For the selected analytes, the quality of the spectral match, as well as the S/N values were comparable between *Set-up II* and *III*. Higher S/N values would be expected for a conventional configuration, because of the sharper peaks generated at faster flow rates. Moreover, within the experimental conditions applied here, the ^{2}D peak widths generated were comparable (**Table 2**) and in accordance with the results recently obtained by Tranchida *et al.* [29].

Data reported in **Table 3** also show that the GC×2GC-MS/FID platform provides enhanced information, because the concurrent presence of two detectors not only provides contemporary analyte identification and quantitation, but also offers internal cross-validation of results. It is also important to note that the international guidelines for quantitative gas chromatography of volatile flavoring substances and essential oils [30-32] indicate Relative Response Factors (*RRF*) (i.e. external standard calibration with internal standard normalization) as the most suitable approach to obtain consistent quantitative data in these matrices, in particular with MS detection. However, for complex samples consisting of hundreds of potentially informative peaks, a full quantitative assessment by *RRFs* cannot be applied in practice. The internal normalization approach performed on the FID signal, also known as analyte percent normalization [31], is therefore accepted. In this case, the composition error is minimized by an appropriate selection of internal standard(s) and FID response factors [33-35] making true quantitation by *RRF* necessary only for those compounds that are limited by law (e.g. α- and β-thujone). FID also opens the possibility of applying the approach introduced by de Saint Laumer *et al.* [36] where analytes' *RRFs* on FID signal are estimated on the basis of combustion enthalpies. With this approach, target analytes can be quantified through estimated *RRFs,* with accuracy errors limited to a few % points even without external standard calibration. Parallel dual detection thus seems to be very promising for reliable and simple qualitative component identification, and to quantitate markers of complex samples of natural origin.

4. Conclusions

The advantages of using a dual-secondary-column dual-detection system in an integrated platform for GC×GC have been discussed, and some practical aspects concerning the tuning of experimental conditions to obtain consistent separation patterns from both dimensions have been addressed. These systems can operate at close-to-optimal ^{2}D linear velocities, and double the secondary column loading capacity, with positive effects on overall system orthogonality and resolution.

Experimental data also indicate that the GC×2GC-MS/FID system provides consistent results, both in terms of analyte identification (reliability of spectra and MS matching) and quantitation, also affording internal cross-validation of quantitation accuracy.

The choice of different setups, in terms of ^{2}D column dimensions and flow conditions, should take into consideration some critical aspects, including the auxiliary flow correction, which should be compatible with the turbo pumping capacity and the required sensitivity. The outlet pressure correction adopted in the present study was minimal, and compatible with both system-limiting factors.

These data open the way to investigating further applications, where system orthogonality and loading capacity are key-factors for successful separations.

Acknowledgements

This study was supported by Ricerca Finanziata da Università - Fondo per la Ricerca Locale (Ex 60%) Anno 2013.

411

412 **References**

413 1. M. Adahchour, J. Beens, R.J.J. Vreuls, U.A.Th. Brinkman, Recent developments in comprehensive
414 two-dimensional gas chromatography (GC × GC): I. Introduction and instrumental set-up, Trends
415 Anal. Chem. 25 (2006) 438-454.
416 2. H.J. Cortes, B. Winniford, J. Luong, M. Pursch, Comprehensive two dimensional gas
417 chromatography review, J. Sep. Sci. 32 (2009) 883-904.
418 3. C. Cordero, E. Liberto, C. Bicchi, P. Rubiolo, P. Schieberle, S.E. Reichenbach, Q. Tao, Profiling food
419 volatiles by comprehensive two-dimensional gas chromatography coupled with mass spectrometry:
420 Advanced fingerprinting approaches for comparative analysis of the volatile fraction of roasted
421 hazelnuts (*Corylus avellana* L.) from different origins, J. Chromatogr. A. 1217(2010) 5848-5858
422 4. J. Harynuk, T. Górecki, J. de Zeeuw, Overloading of the second-dimension column in comprehensive
423 two-dimensional gas chromatography, J. Chromatogr. A. 1071 (2005) 21-27
424 5. Z. Zhu, J. Harynuk, T. Górecki, The Effect of the First-dimension Column Film Thickness on
425 Comprehensive Two-dimensional Gas Chromatographic Separation, J. Chromatogr. A. 1105 (2006)
426 17-24
427 6. Z. Liu, J. B. Phillips, Comprehensive two-dimensional gas chromatography using an on-column
428 thermal modulator interface, J. Chromatogr. Sci. 1067 (1991) 227-231
429 7. J. B. Phillips, C. J. Venkatramani, Comprehensive two-dimensional gas chromatography applied to
430 the analysis of complex mixtures, J. Microcolumn Sep. 5 (1993) 511-516
431 8. P. Q. Tranchida, A. Casilli, P. Dugo, G. Dugo, L. Mondello, Generation of improved gas linear
432 velocities in a comprehensive two-dimensional gas chromatography system, Anal. Chem. 79 (2007)
433 2266-2275
434 9. J. Harynuk, T. Gorecki, Comprehensive two-dimensional gas chromatography in stop-flow mode, J.
435 Sep. Sci. 27 (2004) 431-441.
436 10. J. Harynuk, T. Gorecki, Comparison of comprehensive two-dimensional gas chromatography in
437 conventional and stop-flow modes, J. Chromatogr. A 1105 (2006) 159-167.
438 11. N. Oldridge, O. Panic, T. Gorecki, Stop-flow comprehensive two-dimensional gas chromatography
439 with pneumatic switching, J. Sep. Sci. 31 (2008) 3375-3384.
440 12. M. M. Koek, B. Muilwijk, L.L.P. van Stee, T. Hankemeier, Higher mass loadability in comprehensive
441 two-dimensional gas chromatography-mass spectrometry for improved analytical performance in
442 metabolomics analysis, J. Chromatogr. A. 1186 (2008) 420-429
443 13. C. Cordero, C. Bicchi, M. Galli, S. Galli, P. Rubiolo, Evaluation of different internal-diameter column
444 combinations in comprehensive two-dimensional gas chromatography in flavour and fragrance
445 analysis, J. Sep. Sci. 31 (2008) 3437-3450

14. D. Peroni, R.J. Vonk, W. van Egmond, H.-G. Janssen, Macroporous polymer monoliths as second dimension columns in comprehensive two-dimensional gas chromatography: a feasibility study, J. Chromatogr. A 1268 (2012) 139-149
15. D. Peroni, A.A.S. Sampat, W. van Egmond, S. de Koning, J. Cochran, R. Lautamo, H.-G. Janssen, Comprehensive two-dimensional gas chromatography with a multi-capillary second dimension: A new column-set format for simultaneous optimum linear velocity operation, J. Chromatogr. A 1317 (2013) 3-11
16. D. Peroni, H-G. Janssen, Comprehensive two-dimensional gas chromatography under high outlet pressure conditions: a new approach to correct the flow-mismatch issue in the two dimensions, Journal of Chromatography A, 1332 (2014) 57–63
17. P.Q. Tranchida, M. Zoccali, F.A. Franchina, A .Cotroneo, P. Dugo, L. Mondello, Gas velocity at the point of re-injection: an additional parameter in comprehensive two-dimensional gas chromatography optimization, J. Chromatogr. A. 1314 (2013) 216-223
18. R. Shellie, P. Marriott, P. Morrison, L. Mondello, Effects of pressure drop on absolute retention matching in comprehensive two-dimensional gas chromatography, J. Sep. Sci. 27 (2004) 504-512
19. European Directorate for the Quality of Medicines (EDQM). European Pharmacopoeia VIII ed. 2014
20. C.Bicchi, G. M. Nano, C.Frattini, On the composition of the essential oils of *Artemisia genepı`* Weber and *Artemisia umbelliformis* Lam.,Z. Lebensm. Unters. Forsch. 175 (1982) 182-185
21. J. Beens, H. G. Janssen, M. Adahchour, U. A. Th. Brinkman, Flow regime at ambient outlet pressure and its influence in comprehensive two-dimensional gas chromatography, J. Chromatogr. A. 1086 (2005) 141-150
22. C. Schutjes, P. Leclercq, J. Rijks, C. Cramers, C. Vidalmadjar, G. Guiochon, Model describing the role of the pressure gradient on efficiency and speed of analysis in capillary gas chromatography, J. Chromatogr. 289 (1984) 163-170
23. S.E. Reichenbach, X. Tian, C. Cordero, Q. Tao, Features for non-targeted cross-sample analysis with comprehensive two-dimensional chromatography, J. Chromatogr. A 1226 (2012) 140- 148
24. M. Mucciarelli, M. Maffei, Introduction to the genus. In Medicinal and Aromatic Plants—Industrial Profiles: Artemisia; Wright, C. W., Ed.; Taylor and Francis: London, U.K., 2002; pp 1− 50. Open URL UNIV STUDI DI TORINO
25. P. Rubiolo, M. Matteodo, C. Bicchi, G. Appendino, G. Gnavi, C. Bertea, M. Maffei, Chemical and Biomolecular Characterization of *Artemisia umbelliformis* Lam., an Important Ingredient of the Alpine Liqueur "Genepı`"J. Agric. Food Chem., 57 (2009) 3436-3443
26. D. W. Lachenmeier, D. Nathan-Maister, T. A. Breaux, E. M. Sohnius, K. Schoeberl, T. Kuballa, Chemical composition of vintage preban absinthe with special reference to thujone, fenchone,

pinocamphone,methanol, copper, and antimony concentrations, J. Agric. Food Chem. 56 (2008) 3073-3081

27. Council Directive (EC) No 1334/2008 on on flavourings and certain food ingredients with flavouring properties for use in and on foods and amending Council Regulation (EEC) No 1601/91, Regulations (EC) No 2232/96 and (EC) No 110/2008 and Directive 2000/13/EC.
28. Robert P. Adams, Identification of Essential Oil Components by Gas Chromatography/Mass Spectrometry, 4th Edition, Allured books
29. P.Q. Tranchida, M. Zoccali, F.A. Franchina, P. Dugo, L. Mondello, Measurement of fundamental chromatography parameters in conventional and split-flow comprehensive two-dimensional gas chromatography-mass spectrometry: A focus on the importance of second-dimension injection efficiency, J Sep. Sci. 36 (2013) 212-218
30. IOFI. Analytical procedure for a general quantitative method using coupled capillary gas chromatography/mass spectrometry with selected ion monitoring (SIM). Z. Lebensm.-Unters.-Forsch. 1997, 204, 395.
31. ISO. Essential oils – Analysis by gas chromatography on capillary columns – General methods. International standard ISO 7609, International Organization for Standardization, Geneva, 1985
32. Recommended Practice Flavour Fragr. J. 26 (2011) 297
33. R. Costa, M.R. De Fina, M.R. Valentino, A. Rustaiyan, P. Dugo, G. Dugo, An investigation on the volatile composition of some Artemisia species from Iran, Flavour Fragr. J. 24 (2009) 75-82
34. C. Bicchi, E. Liberto, M. Matteodo, B. Sgorbini, L. Mondello,B. d'Acampora Zellner, Quantitative analysis of essential oils: a complex task, Flavour Fragr. J. 23 (2008) 382-391
35. R. Costa, B. d'Acampora Zellner, M. L. Crupi, M. R. De Fina,M. R. Valentino, P. Dugo, G. Dugo, L. Mondello, GC–MS, GC–O and enantio–GC investigation of the essential oil of *Tarchonanthus camphoratus* L., Flavour Fragr. J., 23 (2008) 40-48
36. J.Y. de Saint Laumer, E. Cicchetti, P. Merle, J. Egger, A. Chaintreau, Quantification in Gas Chromatography: Prediction of Flame Ionization Detector Response Factors from Combustion Enthalpies and Molecular Structures, Anal. Chem. 82 (2010) 6457-6462

Caption to Figures

Figure 1: 2D plots (upper part) and raw chromatograms of *n*-C13-*n*-C15 linear hydrocarbons, analyzed in isothermal conditions at 150°C, 296 kPa head-pressure and 5s of modulation period. **1a:** *Set-up I*; **1b:** *Set-up II* with the outlet pressure correction as indicated in the text.

Figure 2: 2D plots of *Artemisia umbelliformis* essential oil, analyzed with *Set-up I* (**2a** full scan MS and **2b** FID signals), Set-up II (**2c** full scan MS and **2d** FID signals) and Set-up III (**2e** full scan MS and **2f** FID signals). Chemical classes: *m*: mono-terpene hydrocarbons, *s:* sesqui-terpenene hydrocabons, *mox:* oxygenated monoterpenoids, *sox:* oxygenated sesquiterpenoids, *mest:* mono terpenoid esters.

Figure 3: ^{2}D retention time absolute differences (FID *vs.* MS) for: **3a**: *n-alkanes* from *n*-C9 to *n*-C25, **3b**: fourteen volatiles of interest for the flavor and fragrance field.

Figure 4: ^{1}D (**4a**) and ^{2}D (**4b**) retention time variations for *Set-up I*, *Set-up II* (with and without outlet pressure correction) and *Set-up III.*

Figure 5: 2D plots of *Artemisia umbelliformis* essential oil, the magnified region corresponds to the elution area of 2-methylbutyl isovalerate, nonanal and α-thujone. **5a**: the separation pattern obtained from *Set-up II*, and the corresponding raw chromatogram, **5b:** *Set-up III* separation. Apparent resolution values are reported in the text.

Caption to Tables

Table 1: Column configurations, column head pressure (p_i) and midpoint pressure (i.e., estimated pressure at the junction between the 1D column and the two secondary columns - p_z), estimated linear velocities in the ^{1}D and two ^{2}Ds ($^1\bar{u}$, $^2\bar{u}_{MS,}$ $^2\bar{u}_{FID}$), hold-up times and calculated split-ratio.

Table 2: ^{1}D (min) and ^{2}D (sec) retention times, ^{2}D absolute errors (sec), half-height peak-width (ms), number of scans/points per (modulated) peak, normalized 2D Volumes (normalization on geranyl acetate) obtained by analyzing the FFStd2 model mixture with *Set-up II* and *Set-up III*.

Table 3: *Artemisia umbelliformis* essential oil target analytes listed, together with experimental and tabulated [28] Linear Retention Indices in the ^{1}D (I^T_S), MS match factors resulting from the NIST Identity Spectrum Search algorithm, Signal-to-Noise values (Peak-to-Peak S/N as calculated by the Agilent algorithm - SNR) estimated on the highest modulation of each 2D peak, Normalized 2D Volumes (normalization was done on the Internal Standard n-C12) for *Set-ups II* and *III*.

Table 1

	^{1}D column	^{2}D column(s)	Carrier gas (He)[a]	
				Auxiliary EPC correction
Set-up I	30 m, 0.25 mm d_c, 0.25 µm d_f SE52 (95% polydimethylsiloxane, 5% phenyl) Mega (Legnano, Milan, Italy)	to MS detector: 1.6 m - to FID detector: 1.4 m column dimensions: 0.1 mm d_c, 0.10 µm d_f OV1701 (86% polydimethylsiloxane, 7% phenyl, 7% cyanopropyl) Mega (Legnano, Milan, Italy)	p_i: 296.0 KPa p_2: 182.6 KPa $^1\bar{u}$: 34.3 cm/s $^2\bar{u}_{MS}$: 195 - hold-up: 0.8 s $^2\bar{u}_{FID}$: 178 - hold-up: 0.8 s split ratio (MS/FID): 50:50	
Set-up II	30 m, 0.25 mm d_c, 0.25 µm d_f SE52 (95% polydimethylsiloxane, 5% phenyl) Mega (Legnano, Milan, Italy)	to MS detector: 1.4 m - to FID detector: 1.4 m column dimensions: 0.1 mm d_c, 0.10 µm d_f OV1701 (86% polydimethylsiloxane, 7% phenyl, 7% cyanopropyl) deactivated capillary to MS detector: 0.17 m, 0.1 mm d_c Mega (Legnano, Milan, Italy)	p_i: 296.0 KPa p_2: 181.9 KPa p_{aux}: off $^1\bar{u}$: 34.5 cm/s $^2\bar{u}_{MS}$: 198 - hold-up: 0.8 s $^2\bar{u}_{FID}$: 177 - hold-up: 0.8 s split ratio (MS/FID): 51:49	p_i: 296.0 KPa p_2: 182.6 KPa p_{aux}: 39.9 KPa (relative) $^1\bar{u}$: 34.2 cm/s $^2\bar{u}_{MS}$: 180 - hold-up: 0.8 s $^2\bar{u}_{FID}$: 180 - hold-up: 0.8 s split ratio (MS/FID): 50:50
Set-up III	30 m, 0.25 mm d_c, 0.25 µm d_f SE52 (95% polydimethylsiloxane, 5% phenyl) Mega (Legnano, Milan, Italy)	column dimensions: 1.4 m, 0.1 mm d_c, 0.10 µm d_f OV1701 (86% polydimethylsiloxane, 7% phenyl, 7% cyanopropyl) deactivated capillaries for effluent splitting to parallel detectors: to MS detector: 0.4 m, 0.1 mm d_c - to FID detector: 0.25 m, 0.1 mm d_c Mega (Legnano, Milan, Italy)	p_i: 280.0 KPa p_2: 205.1 KPa $^1\bar{u}$: 22.8 cm/s $^2\bar{u}$: 240 - hold-up: 0.6 s split ratio (MS/FID): 50:50	

[a]: reported values were calculated on the basis of reference equations and are just approximations of real ones

Table 2

	Set-up II									***Set-up III***							
	MS (TIC signal)						**FID signal**			**MS (TIC signal)**					**FID signal**		
Compound Name	^{1}D (min)	^{2}D (sec)	^{2}D Error (sec)	Half height pw (ms)	Number of scans	Norm 2D Volume	Half height pw (ms)	Points per peak	Norm 2D Volume	^{1}D (min)	^{2}D (sec)	Half height pw (ms)	Number of scans	Norm 2D Volume	Half height pw (ms)	Points per peak	Norm 2D Volume
α-Pinene	8.25	1.58	0.04	60	21	1.468	60	144	1.358	11.92	1.27	60	14	1.36	60	79	1.153
Benzaldehyde	9.34	2.61	0.02	120	19	0.757	60	89	0.898	13.17	2.02	120	15	0.462	60	115	0.563
Benzyl Alcohol	12.34	3.71	-0.02	180	27	0.424	120	162	0.860	16.42	2.78	180	23	0.428	120	158	0.726
α-Thujone	15.42	2.68	0.00	120	27	0.993	60	113	1.002	19.84	2.02	120	21	0.871	120	86	0.903
Camphor	17.25	2.86	-0.01	120	20	1.400	120	162	1.280	21.84	2.10	120	16	1.160	120	99	1.152
Carvone	21.75	3.05	-0.02	120	23	0.543	120	207	0.801	26.34	2.26	120	19	0.535	120	115	0.707
Cinnamyl Alcohol	24.84	4.10	-0.20	180	27	0.070	120	297	0.473	29.17	2.86	180	26	0.057	120	252	0.379
Geranyl acetate	27.67	2.57	-0.04	120	30	1.000	60	126	1.000	32.17	1.90	120	29	1.000	60	86	1.000
Vanillin	28.50	4.81	-0.13	180	25	0.155	180	207	0.831	33.09	3.45	240	31	0.126	180	209	0.551
Coumarin	30.09	4.62	-0.18	180	33	0.241	120	144	0.823	34.92	3.33	240	29	0.187	120	187	0.541
Isoeugenol	30.59	3.57	-0.12	120	23	0.372	120	279	0.809	35.25	2.54	180	36	0.256	120	125	0.716
Isoeugenyl acetate	36.92	3.71	-0.11	120	21	0.481	120	225	0.693	41.5	2.66	120	21	0.438	120	101	0.791
Benzyl Benzoate	42.75	3.12	0.02	120	56	0.475	120	234	0.710	47.59	2.42	180	29	0.425	120	259	0.799
Sclareol	57.09	3.40	-0.01	180	41	0.828	120	153	1.273	61.92	2.62	240	31	0.530	120	145	1.179

Table 3

				Set-up II		*Set-up III*		*Set-up II*	*Set-up III*	*Set-up II*	*Set-up III*
#ID	**Compound Name**	***Exp.* I^T_S**	***Ref.* I^T_S**[a]	**MS Match Factor**	**SNR**	**MS Match Factor**	**SNR**	**Norm 2D Volume MS (TIC) signal**		**Norm 2D Volume FID signal**	
1	Thujene	918	931	884	3740	906	3433	0.452	0.552	0.242	0.249
2	α-Pinene	925	939	860	12791	833	12232	0.542	0.746	0.666	0.679
3	Camphene	941	953	909	4170	913	3828	0.910	0.978	0.356	0.367
4	Sabinene	966	976	874	63223	893	53153	5.757	5.830	3.477	3.548
5	β-Pinene	970	980	892	44034	889	40563	9.521	9.150	4.063	4.190
6	β-Myrcene	984	991	905	10080	901	9252	2.023	2.185	0.802	0.825
7	p-Cymene	1021	1026	917	59306	915	49859	12.652	15.281	6.166	6.358
8	Limonene	1025	1031	913	3965	927	3640	0.472	0.509	0.271	0.280
9	1,8-Cineole	1029	1033	907	88187	892	84336	47.829	51.810	19.558	20.169
10	γ-Terpinene	1056	1062	853	17482	875	16046	1.900	2.856	1.513	2.259
11	*cis*-Sabinenehydrate	1067	1068	883	9225	869	7755	2.282	3.878	1.654	1.706
12	α-Terpinolene	1085	1088	865	4416	870	4054	0.750	0.861	0.475	0.489
13	2-Methylbutyl isovalerate	1111	1109	912	1264	-	-	0.001	-	0.367	-
14	α-Thujone	1111	1102	903	63176	890	57988	452.460	482.096	157.457	160.677
15	Nonanal	1113	1098	881	1409	-	-	0.193	-	0.000	-
16	β-Thujone	1120	1114	895	57087	896	52588	135.454	148.909	48.767	49.765
17	*trans*-Pinocarveol	1143	1139	887	4458	-		1.841	-	2.263	-
18	Borneol	1174	1165	891	33002	892	30292	42.580	45.591	14.182	14.625
19	4-Terpineol	1183	1177	900	44096	886	37072	57.102	58.992	15.904	16.400
20	α-Terpineol	1198	1189	913	16567	902	15261	15.234	17.996	4.641	4.736
21	Myrtenal	1198	1193	903	13368	874	12271	21.345	18.852	7.579	7.815
22	7-Methyl-3-octen-2-one	1204	-	843	1165	803	1114	1.248	1.279	0.394	0.403
23	*cis*-Piperitol	1213	1193	859	2035	882	1868	1.134	1.256	0.668	0.689
24	Nerol	1228	1228	807	1355	844	1139	1.826	2.240	0.602	0.619
25	Cuminic aldehyde	1244	1239	861	3089	860	2836	2.294	2.263	1.025	1.057
26	Bornyl acetate	1287	1285	910	8634	918[b]	8257	6.243	6.450	1.414	1.458
27	Sabinyl acetate	1293	1291	939	4675	864[b]	4291	1.281	-	1.186	-
28	α-Terpinil acetate	1350	1350	876	29759	879	25019	14.014	15.140	5.269	7.870
29	α-Copaene	1381	1376	896	7647	909	7044	3.616	3.343	1.376	1.419
30	Unknown	1381	-	-	31021	-	28474	15.042	18.534	5.693	5.869
31	Sabinyl isobutyrate	1416	1416	890[c]	65107	912[c]	59761	76.197	71.710	21.347	22.014
32	β-caryophyllene	1425	1418	906	42265	908	40419	23.470	23.208	6.945	7.087
33	*trans*-β-farnesene	1459	1458	871	35327	876	32425	21.491	23.573	6.891	7.106
34	Unknown	1469	-	-	10659	-	9784	5.545	5.772	1.853	1.891
35	Germacrene D	1488	1480	900	21754	881	20804	14.768	14.192	5.276	5.441
36	Biciclogermacrene	1502	1494	869	10547	-	-	7.875	-	1.786	-
37	Sabinyl isovalerianate	1506	1503	906[c]	71628	905[c]	60219	76.137	86.920	39.133	40.355
38	β-bisabolene	1515	1509	890	3808	782	3508	1.745	1.389	0.439	0.453
39	Sabinyl valerianate	1519	1516	892[c]	62671	896[c]	57524	93.136	95.015	27.224	28.074
40	δ-cadinene	1526	1524	846	9409	858	8998	5.033	4.948	1.698	2.536
41	γ-undecalactone	1579	1606	867	1963	902	1802	1.208	1.296	0.560	0.578
42	Spathulenol	1585	1576	874	46948	805[b]	39470	57.990	-	15.830	

43	Neryl isovalerianate	1587	1584	817[c]	60494	896[c]	55527	1.942	112.811	31.251	32.226
44	Caryophyllene oxide	1589	1581	905	28691	890[b]	27437	31.000	84.891	11.036	28.262
45	Unknown	1632	-	-	36098	-	33133	0.098	0.137	15.677	16.167
46	Unknown	1675	-	-	14160	-	11905	25.263	23.381	4.651	4.785
47	γ-dodecalactone	1686	1671	817	1038	854	956	1.294	1.657	0.429	0.442
48	Unknown	1895	-	-	4419	-	4056	3.395	3.374	1.515	1.562
49	Unknown	1918	-	-	14011	-	12861	13.989	14.268	4.327	4.462
50	Unknown MW 232	1951	-	-	10077	-	9637	11.791	12.280	4.034	4.632
51	Unknown	2056	-	-	12421	-	11401	10.115	10.479	3.026	3.120

[a]: Adams Essential Oils database Ref. 28

[b]: partial coelution

[c]: authentic standards ad-hoc synthesized Ref. 25

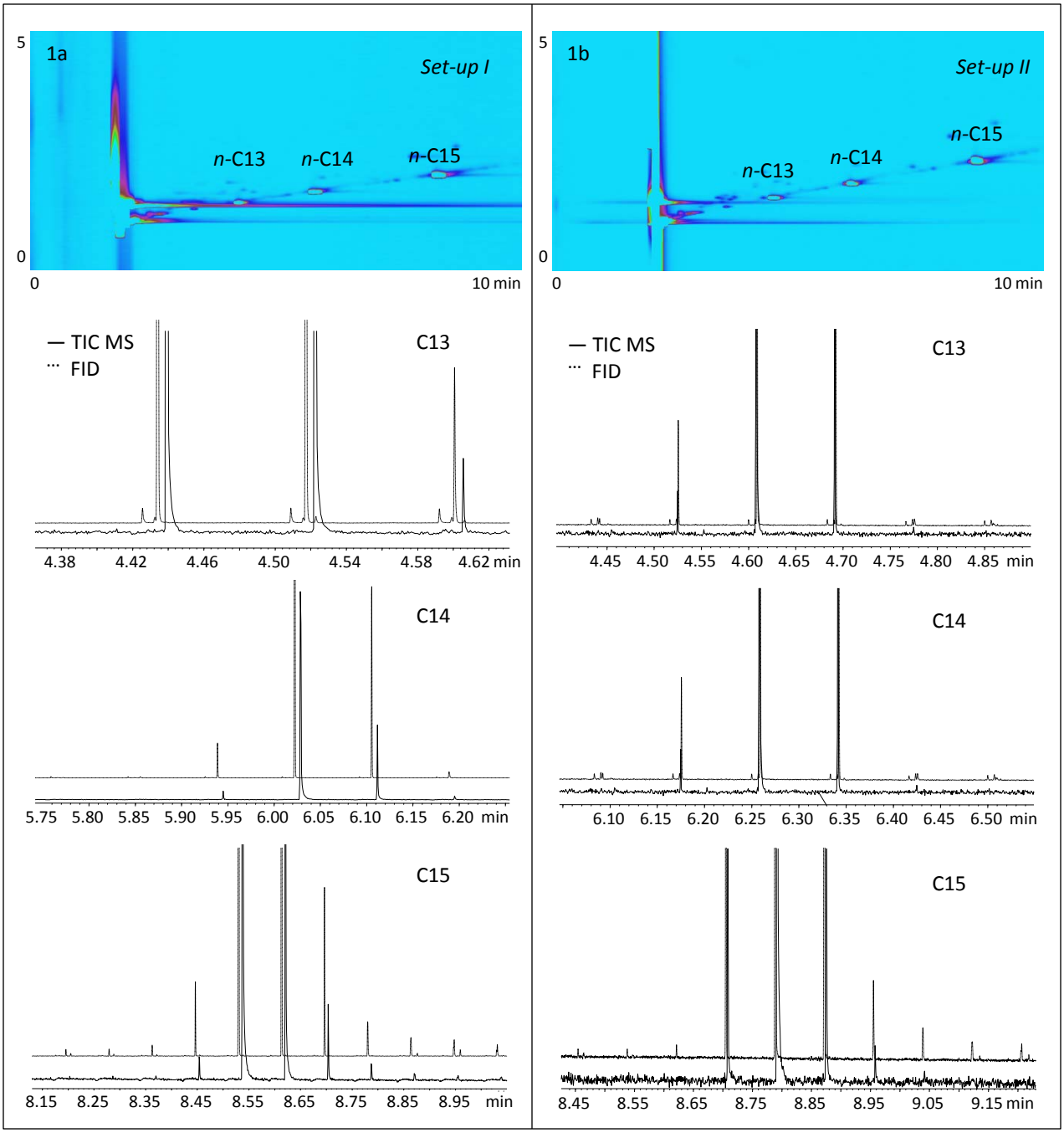
1a
Set-up I
n-C13
n-C14
n-C15
5
0
0
10 min
— TIC MS
··· FID
C13
4.38 4.42 4.46 4.50 4.54 4.58 4.62 min
C14
5.75 5.80 5.85 5.90 5.95 6.00 6.05 6.10 6.15 6.20 min
C15
8.15 8.25 8.35 8.45 8.55 8.65 8.75 8.85 8.95 min
1b
Set-up II
n-C13
n-C14
n-C15
5
0
0
10 min
— TIC MS
··· FID
C13
4.45 4.50 4.55 4.60 4.65 4.70 4.75 4.80 4.85 min
C14
6.10 6.15 6.20 6.25 6.30 6.35 6.40 6.45 6.50 min
C15
8.45 8.55 8.65 8.75 8.85 8.95 9.05 9.15 min

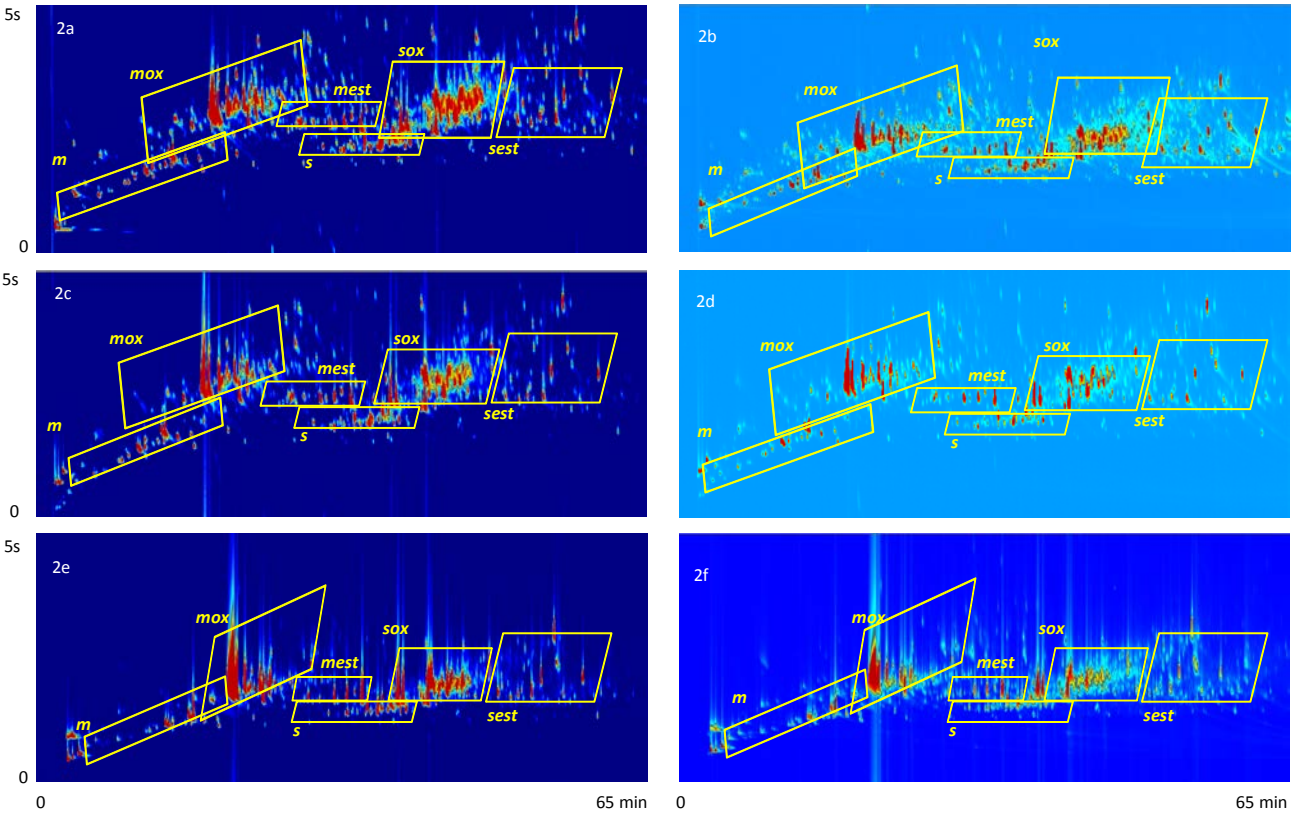
5s
0
2a
mox
sox
mest
m
s
sest
2b
sox
mox
mest
m
s
sest
5s
0
2c
mox
sox
mest
m
s
sest
2d
mox
sox
mest
m
s
sest
5s
0
2e
mox
sox
mest
m
s
sest
2f
mox
sox
mest
m
s
sest
0
65 min
0
65 min

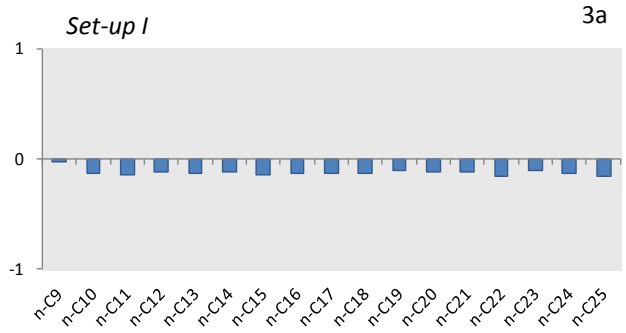
Set-up I
3a
1
0
-1
n-C9
n-C10
n-C11
n-C12
n-C13
n-C14
n-C15
n-C16
n-C17
n-C18
n-C19
n-C20
n-C21
n-C22
n-C23
n-C24
n-C25

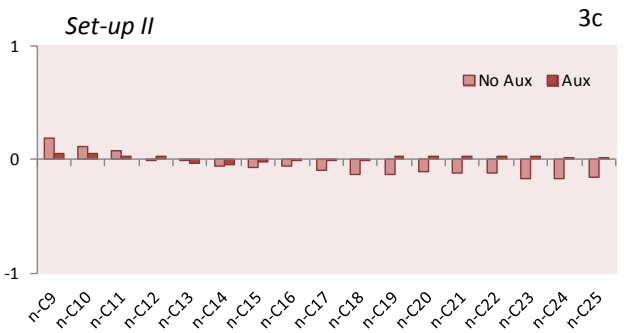
Set-up II
3c
No Aux
Aux
1
0
-1
n-C9
n-C10
n-C11
n-C12
n-C13
n-C14
n-C15
n-C16
n-C17
n-C18
n-C19
n-C20
n-C21
n-C22
n-C23
n-C24
n-C25

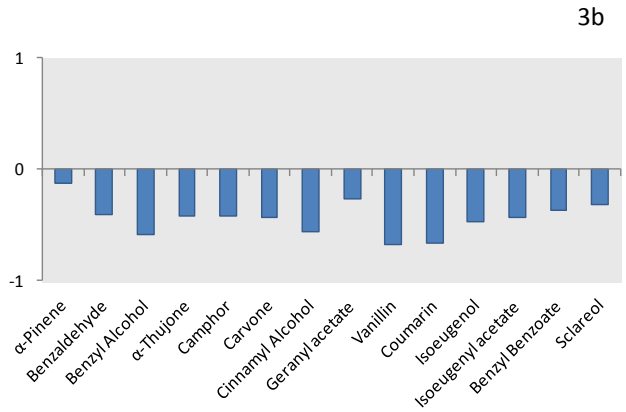
3b
1
0
-1
α-Pinene
Benzaldehyde
Benzyl Alcohol
α-Thujone
Camphor
Carvone
Cinnamyl Alcohol
Geranyl acetate
Vanillin
Coumarin
Isoeugenol
Isoeugenyl acetate
Benzyl Benzoate
Sclareol

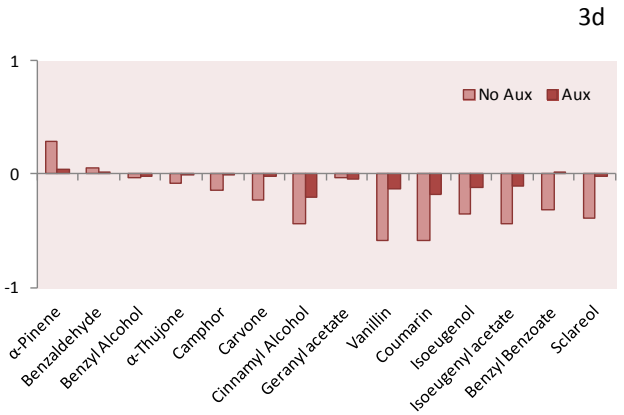
3d
No Aux
Aux
1
0
-1
α-Pinene
Benzaldehyde
Benzyl Alcohol
α-Thujone
Camphor
Carvone
Cinnamyl Alcohol
Geranyl acetate
Vanillin
Coumarin
Isoeugenol
Isoeugenyl acetate
Benzyl Benzoate
Sclareol

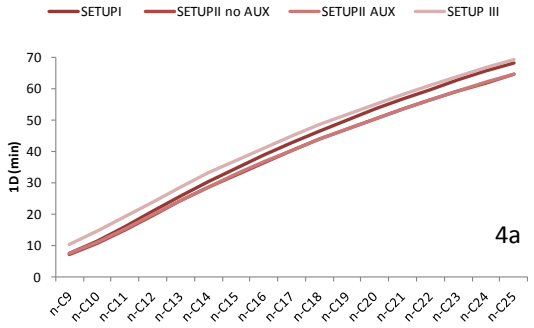
SETUPI
SETUPII no AUX
SETUPII AUX
SETUP III
1D (min)
0
10
20
30
40
50
60
70
n-C9
n-C10
n-C11
n-C12
n-C13
n-C14
n-C15
n-C16
n-C17
n-C18
n-C19
n-C20
n-C21
n-C22
n-C23
n-C24
n-C25
4a

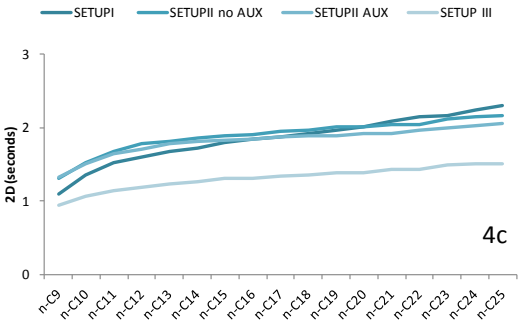
SETUPI
SETUPII no AUX
SETUPII AUX
SETUP III
2D (seconds)
0
1
2
3
n-C9
n-C10
n-C11
n-C12
n-C13
n-C14
n-C15
n-C16
n-C17
n-C18
n-C19
n-C20
n-C21
n-C22
n-C23
n-C24
n-C25
4c

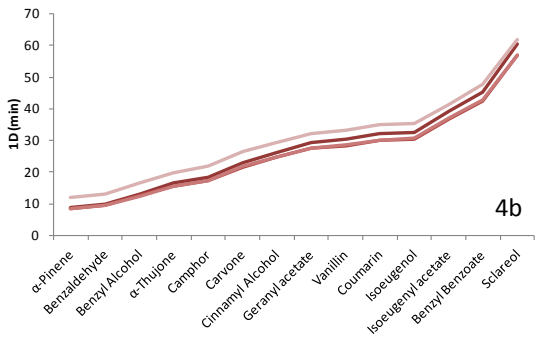
1D (min)
0
10
20
30
40
50
60
70
α-Pinene
Benzaldehyde
Benzyl Alcohol
α-Thujone
Camphor
Carvone
Cinnamyl Alcohol
Geranyl acetate
Vanillin
Coumarin
Isoeugenol
Isoeugenyl acetate
Benzyl Benzoate
Sclareol
4b

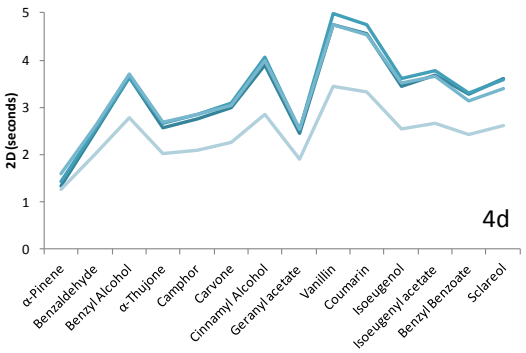
2D (seconds)
0
1
2
3
4
5
α-Pinene
Benzaldehyde
Benzyl Alcohol
α-Thujone
Camphor
Carvone
Cinnamyl Alcohol
Geranyl acetate
Vanillin
Coumarin
Isoeugenol
Isoeugenyl acetate
Benzyl Benzoate
Sclareol
4d

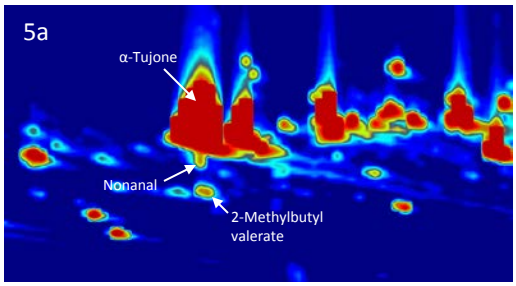
5a
α-Tujone
Nonanal
2-Methylbutyl
valerate

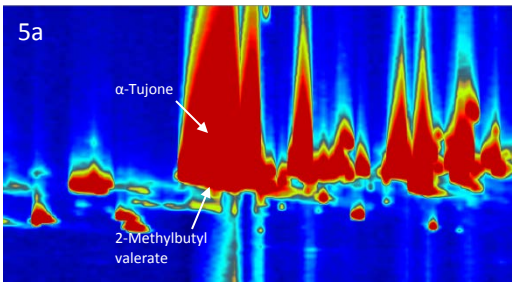
5a
α-Tujone
2-Methylbutyl
valerate

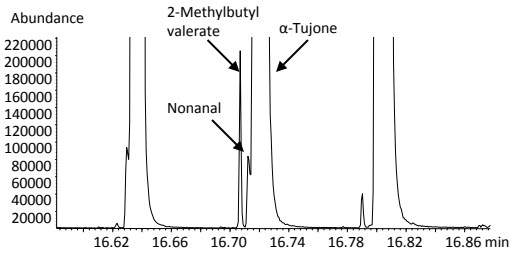
Abundance
2-Methylbutyl
valerate
α-Tujone
Nonanal
220000
200000
180000
160000
140000
120000
100000
80000
60000
40000
20000
16.62
16.66
16.70
16.74
16.78
16.82
16.86 min

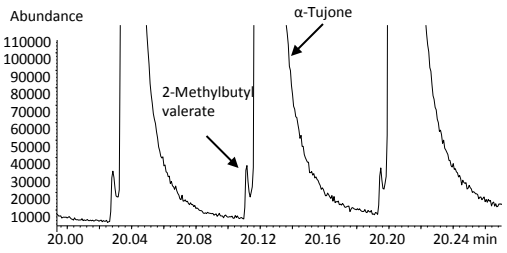
Abundance
α-Tujone
2-Methylbutyl
valerate
110000
100000
90000
80000
70000
60000
50000
40000
30000
20000
10000
20.00
20.04
20.08
20.12
20.16
20.20
20.24 min

1. Loop-Type thermal modulator
(Zoex Corporation, Houston, TX)

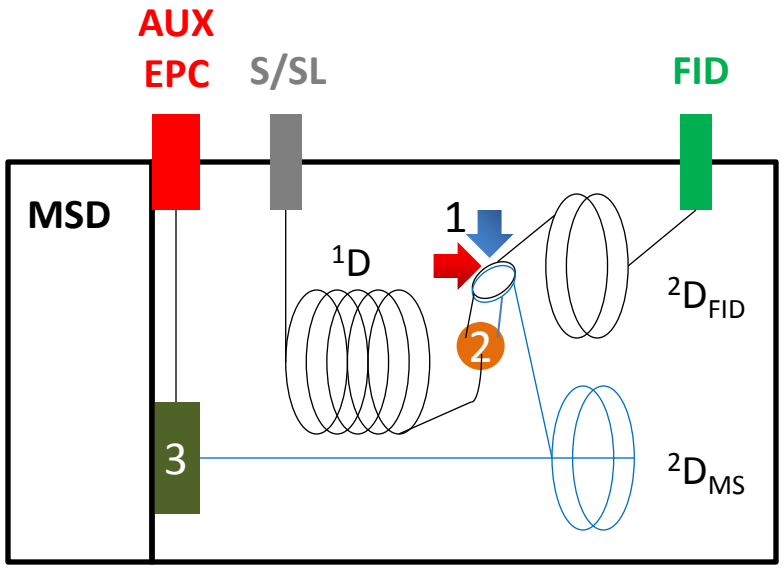

2. Microfluidic 3-port splitter
(Sil-flow™- SGE Ringwood, Victoria, Australia)

3. Outlet pressure compensation
Microfluidic device (Quick-Swap™- Agilent)